DEVELOPMENT OF CONTROL LAWS FOR THE SIMULATION OF A NEW TRANSPORT AIRCRAFT

F. Holzapfel* and O. da Costa*, M. Heller and G. Sachs****
***IABG mbH, Ottobrunn, Germany,**
****Institute of Flight Mechanics and Flight Control, TU München, Germany,**

Keywords: *flight control, transport aircraft, fly-by-wire*

Abstract

This paper presents the development of fly-by-wire control laws used for the high-fidelity simulation of a new transport category aircraft. Beyond structural and gain design aspects for normal operations, also envelope protections and limitations as well as mode transition issues are addressed. As the control system is to be adjusted to changing aircraft datasets at different levels of fidelity, particular emphasis has been put on a high level of automation in gain design and system assessment routines.

1 Introduction

With the availability of significant computing power, numerical simulation has become one of the primary methods to verify the capabilities of a new aircraft design during the stages of its development.

Such efforts are not only of interest to the aircraft manufacturers but also to customers as they can continuously accompany and trace the development of the system and monitor the compliance with the original specifications and requirements based on own and independent simulations.

The restricting factor is the limited amount of data available from the manufacturer that introduces a significant amount of uncertainty into the process.

However, statements concerning tendencies and parameter changes are quite robust and help to properly predict the consequences of configuration changes like new mass and gross weight data, tank volumes, aerodynamic efficiencies, control surface sizing, lever arms, etc. This gives the customer a solid and stable basis for planning his responses and reactions to manufacturer statements.

For modern fly-by-wire aircraft, the dynamic behavior of the system, its operational envelope, its performance and handling characteristics are defined by the flight control system – of course within the physical limits provided by capabilities of the configuration and its subsystems.

As a consequence of this, the proper simulation of the flight control system turns out to be a crucial aspect that must be considered right from the beginning. Especially if flight phases like steep approaches, where the available envelope is fully exploited or in precision tracking tasks, where bandwidth matters, the limitations and characteristics introduced by the FCS may not be neglected for representative analysis results.

As no manufacturer information is available on the internal structure of the flight control system but only on the characteristics as seen from the pilot's point of view, a completely own structural design is to be performed. Thus the FCS layout concerning feedbacks, command paths and filters as well as the implementation of mode transitions has been developed independently from the scratch.

As the design is not performed for a flying aircraft but one under development, where content, amount and fidelity of the data available is subject to rapid change, a high level of automation in system analysis, filter and gain design as well as closed-loop assessment is of high importance to reduce the workload for recurring tasks.

The FCS design presented in the paper has been performed at the Defense Branch of IABG

mbH of Ottobrunn Germany, primarily intended for use in the new research flight simulator of the Institute of Flight Mechanics and Flight Control (LFM) of the Technische Universität München in Munich, Germany.

2 Requirements and Specifications

As the primary purpose of the FCS design is to replicate the functional behavior of a future transport aircraft, all announced and expected features for the configuration under consideration are to be implemented.

2.1 Functional Specification

For the pitch dynamics, the primary specifications are:

- A C* command law providing neutral flight-path stability from the pilot point of view
- Scaling of the C* command to stay within the configuration-specific allowed load factor envelope at full stick deflections
- An angle of attack command law at high angles of attack that prevents the aircraft from overshooting the angle of attack associated to the maximum lift coefficient
- A speed command system for high speeds that allows speed control between maximum operating speed or Mach number and the maximum dive speed without overshooting the commanded value.
- A pitch angle limitation that restricts the steady-state pitch angle to a nominal range, allowing only mild and transient overshoots
- Positive pitch-stiffness during flare to provide natural behavior during landing
- Turn compensation up to a certain bank angle
- Direct elevator and stabilizer control on the ground
- A stabilizer auto-trim function continuously unloading the elevator using the stabilizer; to be frozen during landing, maneuvering or at the edge of the envelope
- Different degraded modes down to direct surface control supported by rudimentary damping feedbacks

As far as the lateral dynamics is concerned, the following requirements exist:

- Stability axis roll rate control for normal bank angles with no sideslip excursions to be produced
- Direct bank angle control for higher bank angles with positive spiral stability up to a given limit bank angle
- Limitation of the maximum achievable steady-state bank angle allowing only small and transient overshoots
- Pedal commands angle of sideslip associated with a small build-up in bank angle
- Decoupling of roll and yaw axis in terms of disturbance response and attenuation
- Proper turn coordination
- Provision of a constant response behavior over the whole envelope
- Positive spiral stability, i.e. direct bank angle control for all bank angles in phases where pitch axis protections are active
- Direct control surface control on the ground
- Different degraded modes down to direct aileron/roll-spoiler and rudder control augmented by rudimentary damping feedbacks

2.2 Design & Implementation Requirements

Easy and quick adaptability to new aircraft datasets, different levels of model fidelity as well as the fast modification of numeric values for handling qualities and limit values for the aircraft envelope are top level requirements of paramount interest for the effort at hand. Thus proper low-level requirements for the actual control design, implementation and assessment have to be derived. These are:

- Parameterization of numeric handling qualities requirements and envelope protection and limitation values as function of altitude (density), Mach number and configuration parameters (mass, flaps, gear, etc.)
- Implementation of automated gain and coefficient design routines for all laws and modes based on linearized plant models
- Implementation of automated assessment routines for linear analysis

- Implementation of routines to automatically generate regular table grid data from coefficients designed in available linearization points for gain scheduling
- Formulation of the gain design routines for dynamic systems of arbitrary order, i.e. not for rigid body approximations to account for sensor, sensor processing and actuation system dynamics
- Modular implementation of the control system components and the mode switching logics; minimization of interdependences
- Automated code-generation and build procedure for rapid prototyping

From both, the functional specification as well as from the design and implementation requirements presented above, detailed requirements concerning handling qualities, mode transitions, implementation and interfacing aspects, etc. have been derived. Military specifications, civilian certification standards as well as company proprietary software development and implementation processes complement the proper formulation of the detailed problem statement and its solution process.

3 Lateral-Directional Control System

The basic layout of the lateral-directional control system is depicted in Fig. 1. It can basically be broken down into four components which are the command shaping and feed-forward path, the proportional integral feedback path, the control allocation and the parallel path for the direct control law which is just augmented by rudimentary damping feedback.

The feedback portion consists of a full state feedback of the lateral-directional rigid body states, i.e. the stability axis roll rate p_S, the stability axis yaw rate r_S, the bank angle Φ and an estimated angle of sideslip $\hat{\beta}$. The proportional feedback is performed by the 2×4 matrix $\mathbf{K}_P$. For the angle of sideslip, an estimate is used as flow angles are considered to be expensive feedback variables due to measurement noise and low measurement bandwidth if not filtered and augmented with inertial measurements. Additionally, integral feedback of the control errors in the bank angle and the angle of sideslip is performed as those two variables are the primary control variables of the inner loop of the lateral-directional control system, i.e. the inner loop is a bank angle, not a roll rate command system. It is to be noted that the integral feedback gain matrix is placed before the error integrators to increase the robustness in the nonlinear implementation of the gain-scheduled control system.

The inputs to the integral error gain matrix consist of the errors between the commanded and the actual bank angle and angle of sideslip respectively. The commanded values Φ_C and β_C are also multiplied by the feedforward matrix $\mathbf{H}_{\phi\beta}$ which is designed to cancel the integrator poles from the over-all command input to output transfer function matrix.

Feedforward matrix, proportional and integral feedbacks are designed for decoupled control of bank angle and angle of sideslip as well as for steady-state accuracy in these two variables.

The three signal strings – feedforward, proportional feedback and integral error feedback are added up to two commanded virtual control variables, a virtual roll and yaw control command. Those virtual commands are transformed to physical control surface deflection commands in the control allocation portion which forms the next element of the lateral control system.

The virtual roll control is designed to produce a pure stability axis rolling moment while the associated yawing moment vanishes; the yaw control produces the opposite effect. The transformation from virtual controls to physical commands for left and right ailerons, left and right asymmetric spoiler deflections as well as for the rudder is performed by flight condition dependent look-up tables.

The third major part of the system is the command-shaping portion, generating the inner-loop commands for Φ_C and β_C from the two pilot inceptors for the lateral-directional dynam-

ics which are the lateral stick deflection δ_ξ and the pedal command δ_ζ. In the normal operating mode, the lateral stick command is scaled to produce the maximum design stability-axis roll rate for a full deflection, while the pedal command is scaled to command the maximum design angle of sideslip when fully deflected. Both, the maximum angle of sideslip and the maximum roll rate are scheduled over the dynamic pressure. The angle of sideslip command path is connected to the roll rate path via a high-pass filter. The purpose of this interconnection is to provide the natural build up of a bank angle in conjunction with the commanded angle of sideslip as pilots are used to this behavior from the inherent dynamics of an uncontrolled aircraft. This characteristic must be actively added as the inner loop of the lateral control system decouples the roll and the yaw axes so the bank angle would remain zero during the buildup of a commanded angle of sideslip.

As the superimposed roll rate command from the lateral stick and the high-pass filtered pedal cross feed could exceed the maximum design roll rate, the total roll-rate command is limited again to the allowed limit rate.

Adding a bank angle dependent roll rate to the pilot commanded roll rate implements both, positive spiral stability when a certain bank angle is exceeded and a limitation of the absolute bank angle [1]. This is accomplished by a linear increase of the $p_C(\Phi)$ from zero at the bank angle at which positive spiral stability is to begin to the negative amount of the maximum allowed roll rate at the limit design bank angle $\Phi_{\lim}$, fully cancelling the roll rate commanded by the pilot and thus not allowing him to increase the bank angle over the limit value.

To this point, the lateral stick command is still interpreted as a roll rate whereas the inner loop was presented to be a bank angle command system. Thus, a PI command filter is used to transform the pilot roll rate command to a desired bank angle [2]. The zero of the command filter cancels the stable spiral pole, while the filter pole is located in the origin of the complex plane. This provides the pilot with the desired neutral spiral stability behavior for bank angles below the threshold value for positive spiral stability whereas the inner loop features strong spiral stability, thus tracking the commanded bank angle with steady-state accuracy and countering external disturbances.

For zero cockpit control deflections and small values of the PI filter integrator below a specified threshold bank angle, the integrator is reset to zero to assist wings-level flight. The integrator reset is immediately stopped for non-zero roll rate command to allow the pilot to also actively control small bank angles.

At this point, steady-trim values are added to the commanded bank angle and the commanded angle of sideslip which can be used to produce offsets from zero for centered controls, e.g. to counter asymmetries. As the sum of the pilot commanded and the trim provided reference value may exceed the allowed limit values, a last command limiting is performed. In case one of the hard pitch dynamics protections, either the angle of attack or the high speed protection is active, the bank angle command generated the way as described above is replaced by a bank angle that is proportional to the lateral stick deflection, leading to positive spiral stability in the stick to bank angle transfer function for all bank angles, replacing the roll rate command by a direct bank angle command. Switching between the two alternative bank angle command sources is performed by linear blending over two seconds upon activation or deactivation of one of the relevant pitch dynamics protections.

Finally, the fourth part of the lateral directional control system consists of the direct command law bypassing the whole command filter. In this case, the lateral stick deflection and the pedal deflection are directly scaled to deflections of the virtual roll and yaw control, augmented by a trim value, which replicates conventional aileron or rudder trim to achieve steady state control surface deflections with centered pilot inceptors. If the direct law is active, those defections are directly fed to the control allocation section with just proportional roll rate feedback added to the roll command and proportional yaw rate feedback added to the

yaw command. All other proportional feedbacks as well as the integral feedbacks and the whole command shaping and feed forward portion of the normal command law are deactivated in this mode.

With the functional structure of the lateral-directional control system illuminated, focus is now on the determination of the available coefficients – the feedback and filter gains, filter coefficients and feed forwards.

The most important numeric requirements for the lateral-directional control system which have been selected for the control design at hand are as follows:

- Dutch roll damping and natural frequency: $1/2\cdot\sqrt{2}$ and 2 rad/s
- Roll Subsidence Mode Time Constant T_R: selected to be very fast
- Spiral Mode Time Constant T_S: Two different philosophies have been pursued – stable and slow and stable and very fast
- Integrator poles: Both selected to be fast – $s_{I,\beta}=-1$ and $s_{I,\phi}=-0.7$
- Modal decoupling: Amplitude ratio $|\phi/\beta|$ in the dutch roll eigenvector to be set to zero
- Roll response criterion $T_{\phi=45°}$ set to a rather crisp value
- Steady state ratio for bank angle command induced by angle of sideslip command: $\phi_{SS}/\beta_{SS}=-1.5$
- Stability requirements: Amplitude margin $A_R=6\,\mathrm{dB}$, phase margin $\phi_R=45°$ for both, roll and yaw loop cut (cut performed at the virtual controls)
- Stability and robustness to be monitored and increased using the smallest singular value of the feedback difference function and the conditioning index $\bar{\sigma}/\underline{\sigma}$ of the closed-loop system matrix

The items detailed above automatically ensure the compliance with other requirements. The modal decoupling eliminates all questions concerning proverse or adverse yaw characteristics or sideslip excursions from roll inputs. The high dutch roll damping also ensures compliance with roll-rate and bank angle oscillation requirements.

For the computation of the feedback gains, eigenstructure assignment is to be used [2, 3, 4, 6, 7]. To correctly place the closed-loop system poles and shape the eigenvectors, it is not sufficient to perform the design process for the rigid-body lateral dynamics alone. The assignment procedure is applied to the full system augmented by the error integrators $x_{I,\beta}, x_{I,\Phi}$ and second order models for aileron $x_\xi, x_{\dot\xi}$, roll-spoiler $x_\zeta, x_{\dot\zeta}$ and rudder actuators $x_{\delta_S}, x_{\dot\delta_S}$. This leads to a linear system with n=12 states, r=2 outputs to be controlled – the bank angle and the angle of sideslip and m=2 control variables – the virtual roll $\delta_{Roll,cmd}$ and yaw the control $\delta_{Yaw,cmd}$.

It is to be mentioned that the linear system may be extended by further states, e.g. sensor, sensor filtering or processing states, elastic modes, etc. without limiting or restricting the applicability of the implemented procedure.

The desired eigenvalues are set to the values detailed above. For the eigenvectors following selections are made with the aim of decoupling the roll and the yaw axis:

- The roll rate and the bank angle entry in the dutch roll eigenvectors are set to zero.
- The yaw rate and the angle of sideslip entries in the eigenvectors of the roll subsidence mode and the spiral mode are set to zero.
- For the integrator modes, the bank angle entry in eigenvector for the bank angle mode is set to one whereas the angle of sideslip entry is set to zero. For the angle of sideslip mode, the opposite procedure is performed.
- As only two controls are available, only two eigenvector elements may be specified. Thus the entries of the eigenvectors not mentioned above are marked as non-relevant so the degrees of freedom available for influencing the eigenvectors are not wasted for unimportant elements.

As far as the control allocation algorithm is concerned, the distribution from virtual roll and yaw controls to physical surface deflections is

computed based on weighted generalized pseudo-inverses. If the commanded physical control vector consisting of aileron, roll spoiler and rudder deflections is $\mathbf{u}_{lat}$ while the virtual control vector is $\bar{\mathbf{u}}_{lat}$, then the allocation matrix $\mathbf{K}_{Alloc,lat}$ mapping $\bar{\mathbf{u}}_{lat}$ to $\mathbf{u}_{lat}$ by $\mathbf{u}_{lat} = \mathbf{K}_{Alloc,lat} \cdot \bar{\mathbf{u}}_{lat}$ must satisfy

$$\begin{bmatrix} L_\xi & L_\zeta & L_{\delta_S} \\ N_\xi & N_\zeta & N_{\delta_S} \end{bmatrix} \cdot \mathbf{K}_{Alloc,lat} = \begin{bmatrix} 1 & 0 \\ 0 & 1 \end{bmatrix} \quad (1)$$

As this equation features an infinite number of solutions, the use of the three control surfaces can be relatively weighted by a 3×3 positive definite weighting matrix $\mathbf{W}_{Alloc,lat}$ where higher values stand for increasing the utilization of the corresponding control surface.

The resulting control allocation matrix is determined using

$$\mathbf{K}_{Alloc,lat} = \mathbf{W}_{Alloc,lat}^{-1} \cdot \mathbf{B}_{lat}^{T} \cdot \left(\mathbf{B}_{lat} \cdot \mathbf{W}_{Alloc,lat}^{-1} \cdot \mathbf{B}_{lat}^{T} \right) \quad (2)$$

If moment demands cannot be produced by the allocation scheme provided by $\mathbf{K}_{Alloc,lat}$ as control surfaces start to saturate, the remaining moment demand is redistributed to the non-saturated surfaces. In this case however, the decoupling property of the controls is lost.

The feed forward matrix $\mathbf{H}_{\phi\beta}$ is computed to cancel the two poles introduced by the error integrators so those are not visible in the stick/pedal to bank/sideslip transfer functions.

In the PI bank angle command filter, the integral gain is set to one and the transfer function zero is placed to cancel the stable spiral mode of the inner loop producing neutral spiral stability in the stick to bank transfer function when the absolute bank angle is below the threshold value. A detailed description of the lateral-directional control system can be taken from [8].

4 Pitch Axis Control System

The basic layout of the pitch axis control system is depicted in Fig. 2. This portion of the system features multiple limitation and protection modes requiring transient free blending.

The inner loop of the longitudinal FCS portion controls the stability frame normal load factor $n_{Z,S}$ (as to be detailed later, the load factor signal used for feedback is modified). To accomplish that, the pitch rate and the normal load factor are used in proportional feedbacks, while an additional integral feedback of the load factor error is used to provide steady state accuracy. The feed forward gain h_{n_Z} is selected to cancel the error integrator pole from the stick to load factor transfer function.

The command input to the inner loop core thus is a load factor increment $\Delta n_{Z,S}$ to the current trim condition that is represented by linear flight trajectory at a given flight path angle and flight path bank angle.

As the pilot is required to command C* in normal flight whereas the inner loop controls the load factor, the pitch stick input must be shaped in a way that full forward and aft deflections always correspond to the absolute limit values for the normal load factor which is allowed for the current flight condition and configuration (considering gear, flap position, etc.). Thus the normalized stick command is linearly scaled from $[-1,0,1]$ to $[C^*_{\min},0,C^*_{\max}]$ with

$$C^*_{\min/\max} = \left(1 + \frac{V_m}{V}\right) \cdot \left(n_{Z,\min/\max} - n_{Z,Trim}\right) - \Delta n_{Z,Turn} \quad (3)$$

Here, V_m is the C* blending speed weighting between pitch rate and load factor contribution to C*. It is to be mentioned that this computation is based on the quasi-steady-state relationship between linear system load factor and pitch rate response.

Then, the pilot C^* command is converted into an equivalent $\Delta n_{Z,S}$ pilot command by

$$\Delta n_{Z,S,C,Pilot} = C^* / \left(1 + V_m / V\right) \quad (4)$$

The total commanded load factor difference also includes the turn compensation component $\Delta n_{Z,Turn}$ which compensates the rotation of the lift vector out of the horizontal plane up to a certain flight path bank angle, eliminating the need for the pilot to apply additional back pressure on the pitch control to maintain the current flight-path angle.

The absolute load factor also contains the trim load factor $n_{Z,Trim}$. As structural limitations do not apply to load factor increments but to the absolute value of the normal load factor, the resulting command value for the absolute normal load factor must be computed before command limiting can be performed:

$$n_{Z,S,C} = \Delta n_{Z,S,C,Pilot} + \Delta n_{Z,Turn} + n_{Z,Trim} \qquad (5)$$

This value is clipped to account for the configuration dependent load factor limitations of the aircraft. After that, the trim value is deducted again to produce the $\Delta n_{Z,S}$ command value required as command input for the inner loop.

For the further processing of the command value, two different approaches have been pursued. One method is to directly forward the unmodified $\Delta n_{Z,S}$ command to the protection limiter. The other way is to feed the command signal through a shaping filter consisting of two sequential lead-lag shaping filters. The purpose of those shaping filters is to reduce or eliminate the attitude drop back by modifying the $T_{\Theta 2}$ zero in the stick to attitude transfer function. The payoff in diminishing the attitude drop back is, however, a reduced bandwidth in the stick to flight-path angle transfer function. The shaping filters reduce the pitch rate overshoot q_{peak}/q_{SS} in the stick to pitch rate transfer function. This functionality could also be achieved with one lead lag filter alone. The second lead lag filter is required to accelerate the initial response to a stick deflection to restore the CAP parameter as the pilot expects a proper correlation between the initial pitch rate acceleration and the resulting quasi-steady load factor response which is the interpretation of CAP.

A very important aspect of the control design at hand is that the intervention of envelope protections and limitations is implemented by dynamic limiters to the upper and lower bound value of the normal command path $\Delta n_{Z,S}$. This means, if a protection or limitation requires a $\Delta n_{Z,S}$ smaller than that currently commanded by the pilot, the command value is reduced to the value provided by the limitation / protection. The same holds on the lower side. By that procedure, it is ensured that no transients occur when a protection becomes active on one side and on the other side, the protection stops to interfere with the pilot command as soon as the load factor increment commanded by the pilot no longer corresponds to a flight condition out of the protected envelope.

It is to note that when designing the different protection modes, the control variable available to the related feedback loops is no longer the elevator or a pitch control surface but a $\Delta n_{Z,S}$ command. The feedback philosophies of the pitch axis protections and limitations will be described later in this section.

In the normal C* operation mode, the command value for $\Delta n_{Z,S}$ computed so far is on the one hand fed-forward to the pitch control command after multiplication with the feed forward gain h_{n_z} and on the other hand used to compute the control error for the integral feedback of the normal load factor in the stability frame. The main purpose of the integral feedback is to provide steady-state accuracy. The multiplication of the error signal with the integral error feedback gain k_{I,n_Z} is performed before the integration.

The output of the inner control loop is a elevator deflection command consisting of a superposition of the feed-forward, the integral load factor feedback and the proportional feedback of the load factor and the pitch rate. It is on the one hand directly sent to the elevator actuator and on the other hand slowly integrated to a stabilizer deflection. This procedure continuously slowly moves the elevator back to zero deflection by producing the trim moment required for steady-state flight conditions by the stabilizer. During transient flight maneuvers and in protections, stabilizer integration is frozen as those conditions are not to be trimmed as steady states.

So far, the descriptions have addressed the normal operation mode, i.e. the aircraft is in normal flight and none of the envelope limitations and protections are active. While mode

activation criteria and transition / switching logics are to be detailed later, the system structure of the different protection modes and flight laws is presented in the following sections in form of changes to the normal operating law and mode.

In the direct control law, the whole feed forward branch including the command shaping and limiting portions is bypassed and replaced by a direct mapping of pitch stick to elevator deflections using a look-up table. The manual elevator deflection command is just augmented by rudimentary proportional load factor and pitch rate feedback to ensure sufficient short period damping and natural frequency. The stabilizer auto-trim is deactivated in the direct control law, manual stabilizer trim must be performed to eliminate steady-state pitch stick deflections.

The same direct link between pitch stick and elevator is active when the aircraft is on the ground.

During flare, the pitch integrator and the stabilizer are frozen and an additional high pass-filtered speed feedback is introduced. These steps are implemented to generate positive pitch stiffness comparable to an aircraft without a flight control system and thus natural and intuitive behavior during flare and landing. Without those measures, the neutral pitch stability provided by the FCS would eliminate the need for the pilot to continuously apply back pressure during flare and landing and thus require unnatural block-inputs at the pitch stick.

For the pitch angle limitation, the pilot command value for the load factor increment $\Delta n_{Z,S}$ is simply limited by a low-pass filtered feedback of the error between the actual pitch angle and the limit pitch angles. The maximum allowed load factor increment is computed from the upper pitch angle limit, the lower bound for $\Delta n_{Z,S}$ is derived from the minimum pitch angle to be maintained. Thus, at the boundaries of the intended pitch angle envelope, the $\Delta n_{Z,S}$ is limited to zero, allowing only negative values for $\Delta n_{Z,S}$ above the maximum pitch angle and positive values if the nose falls below the minimum permissible attitude. As temporarily exceeding the intended pitch angle range does not pose an immediate danger to the aircraft, slight excursions over the threshold values are allowed, however, it is ensured that the transient overshoots are only small and of short duration. Allowing these overshoots eliminates the need of early control system interference with the pilot commands when the aircraft is still in the permissible pitch attitude region.

As far as the angle of attack is concerned, the high AoA protection again limits the maximum $\Delta n_{Z,S}$ to be commanded by the pilot as a function of the error between a commanded and the actual angle of attack. The commanded α is determined from the pitch stick deflection and ranges from an AoA which is some degrees below the angle of attack for maximum lift for zero deflection up to an angle of attack slightly below the lift curve maximum for full stick aft deflection.

As not exceeding the maximum angle of attack is of crucial interest, no transient overshoots are allowed. Thus the angle of attack feedback is designed to feature a high bandwidth and to be very responsive. Furthermore, to ensure steady-state accuracy, the integral load factor error feedback is replaced by integral feedback of the angle of attack deviation. Furthermore, the same high-pass filtered speed feedback that has already been addressed in the pitch angle limitation is activated to produce a nose-down moment if the speed is rapidly bleeding and thus to help to avoid transient angle of attack overshoots. Furthermore, the stabilizer is frozen to ensure that it does not produce additional nose-up moments.

The overspeed protection is implemented in analogy to the high angle of attack protection. However, in this case, the load factor is lower bounded by the protection. The commanded velocity is linearly scaled between the maximum operating speed V_{MO} / maximum operating Mach number M_{MO} (whichever results in a smaller indicated air speed) for neutral pitch stick and the dive speed V_D / dive Mach number M_D for pitch stick fully forward. The feedback signal used for the overspeed protection is the

error between the commanded speed and the lead-lag filtered indicated airspeed. When the high speed protection is active, the stabilizer auto-trim is frozen in the direction of nose-down moments to avoid trimming excessive speeds as steady-state flight conditions.

Fig. 3 illustrates the principle of the limitations and protections restricting the range of allowed load factor increments to be commanded by the pilot.

For the pitch axis, the same gain design procedure is used as presented for the lateral directional flight control system. However, no eigenvector specifications are made; just the eigenvalues for the short period mode and the integrator are adressed. The feedforward gain is designed to cancel the load factor integrator zero in normal operation mode.

Additionally, the following considerations have been made to design the gains for the protection and limitation modes:

- The speed feedback used during flare and high angle of attack protection features a gain of $\sqrt{2} \cdot Z_U$, eliminating the phugoid influence from the stick to angle of attack transfer function response.
- For the speed high-pass filter, a time constant of $T = 30\mathbf{s}$ was chosen
- The zero of the lead-lag filter for the overspeed protection is selected to be $T_{1,V} = 1/\omega_{n,Phugoid}$ and the pole of the filter $T_{2,V}$ is selected to cancel the slowest zero of the commanded load factor to speed transfer function. This procedure has the effect that not the phugoid, but the short period branches of the commanded load factor to speed transfer function root locus plot generate the asymptote running into the instable right half of the complex plane, allowing much higher speed feedback gains for tight speed tracking. For the final speed feedback gain of the overspeed protection, the gain value leading to the smallest imaginary part of the short period poles is chosen.
- The position of the pole of the pitch attitude limitation low pass filter is chosen to cancel the zero of the load factor command to pitch attitude transfer function which causes the short period branches of the root locus to decrease the closed-loop damping.

A detailed description of the pitch control system can be taken from [9].

5 Control System Implementation

5.1 Nonlinear Compensations and Couplings

In this section, the aspects concerning couplings between pitch and lateral-directional control system are addressed as well as implementation aspects dealing with the nonlinear dynamics of the plant.

First of all, the stability axis load factor itself is not suitable for feedback as it has to be corrected for the trim contribution of the current flight condition. Thus, the load factor increment to trimmed flight to be used for feedback is computed as

$$\Delta n_{Z,S} = n_{Z,S} - \cos\gamma \cdot \cos\mu \qquad (6)$$

where γ is the flight-path climb angle and μ the flight-path bank angle. The linear system models used for gain design are generated around straight and level flight, where gradients in load factor due to path and bank changes vanish in the system matrix. Thus, the effect of the nonlinear term is not present during gain design but manifests in the flight-path angle slowly drifting away from the steady-state value for non-horizontal flight conditions. The presence of the trim compensation removes this unintended phenomenon. Furthermore, it is also possible to compensate for the change of the trim load factor by means of gravity rate compensation.

The next nonlinear aspect is the turn compensation which produces a load factor increment dependent on the flight-path bank angle that allows maintaining the actual path angle in the vertical plane without a requirement for the pilot to apply additional back pressure. The turn compensation term is computed as

$$\Delta n_{Z,Turn} = \cos\gamma \cdot \left(\sin^2 \mu_{\lim} / \cos\mu_{\lim}\right) \qquad (7)$$

The subscript “lim” indicates that the turn compensation is limited to a certain bank angle in the normal operating range. If the pilot intends to fly coordinated turns at higher bank, the additional load factor must actively be commanded.

The limit values for all relevant control variables are interpolated from tables which are dependent on configuration and flight conditions.

The coefficients of control system filters and feedback gains are scheduled dependent on free stream air density, dynamic pressure as well as estimated aircraft mass and C.G. location. For a later project stage, it is planned to try to increase the robust performance and stability of the system in order to eliminate the necessity of configuration specific scheduling. At least as far as the lateral-directional control system is concerned, promising results have already been produced using multi-model eigenstructure assignment and iterative robustification methods based on singular value criteria and eigenvector orthogonalization.

All command and integration values are limited in the nonlinear implementation of the flight control system to avoid out of range commands and control surface saturation.

Supervisory mode control is performed by finite state diagrams providing following functionalities:

- Flight Phase Moding: Determination of the actual phase, either ground, flight or flare based on ground contact, pitch angle and radio altitude as well as on time intervals for which certain conditions have to apply.
- Flight Control Law Moding: Determination of the main mode which can be fly-by wire or direct law and for the fly-by wire case also for the submode which can be normal operation or a reversionary mode with limited functionalities. In the simulation, the mode selection is not performed based on failure scenarios but actively triggered by the pilot.
- Speed feedback activation/deactivation: Activation of the high-pass filtered speed feedback as a function of the selected command law, the activation status of the angle of attack protection and the current flight phase (speed feedback is active during flare).
- Stabilizer mode: The activation / deactivation of the stabilizer auto-trim function is dependent on the activation status of envelope protections, the current command law, the flight phase and the actual flight condition (transient maneuvering or steady-state).
- Control Variable command: Current active control variable in the pitch and lateral control system dependent on control mode, flight phase and protection activation.

Dependent on the system states listed above and the associated state transitions, the supervisory logics controls mode fadings, resets integrators and blends command and control signals.

5.2 Implementation Process

The flight control system described in the paper is implemented in SIMULINK following formal modeling style guidelines. The supervisory and mode logics are coded in form of Stateflow charts. No numeric values are hard-coded in the models, but are transferred from the Matlab workspace using hierarchical workspace data structures.

Matlab design routines have been implemented to allow the automated generation of gain and coefficient tables from a grid of linearized system models, a handling qualities and control systems requirement definition file and a design settings selection file. This process offers a high level of automation with only little user interaction required. This is crucial for the simulation project as on the one hand, model data and revisions rapidly change and on the other hand it is highly desirable to quickly evaluate the impact of changes in system requirements.

Automated linear assessment routines have been implemented to analyze linear system response in both, time and frequency domain.

For time domain simulations, Real-Time Workshop and Stateflow Coder are used to automatically generate C-Code of both the control system and the supervisory logics and to generate a library from that interim stage that can then be linked to the simulation executable.

At the moment, the library is linked to a FORTRAN based simulation model which is to be replaced by an all SIMULINK model currently under development.

6 Assessment

An analysis of the closed-loop dynamics based on the grid of linearized plant models is automatically performed to analyze the efficiency of the gain design process and to monitor the compliance of the resulting behavior with the design requirements.

As an example of the linear assessment, Fig. 4 shows the linear response of the lateral-directional states to steps in bank angle and angle of sideslip command. The time histories proof the quality of the decoupling between roll and yaw axis as for the bank angle command in the left column, no visible angle of sideslip is built-up. The same holds for the sideslip command in the right column, where the bank angle resulting from the sideslip command is negligible. Furthermore, it is clearly visible that the linear dynamics of the closed-loop system reacts in compliance with the handling qualities criteria defined for the system. The roll rate rapidly builds up with the crisp roll time constant specified for the system and the commanded bank angle is achieved aperiodically with the fast and stable spiral mode time constant specified for the inner loop. In the step response for the angle of sideslip, it is clearly visible that the latter one builds up with the required natural frequency and a light intentional overshoot related to the specified relative damping coefficient of $1/2 \cdot \sqrt{2}$.

The linear assessment includes the following system characteristics for both lateral and pitch control loops:

- Command and inner loop variable step responses for all command laws and modes as well as for envelope protections and limitations. State responses are analyzed for decoupling, transient dynamics and steady-state accuracy. Control and control rate responses are monitored for required control deflection budgets as well as control and rate saturation and to judge the over-all control activity
- State variable initial value excursions for the inner loop controllers to analyze disturbance rejection in all states, as well as the associated control activity in terms of absolute control deflections and deflection rates
- Nichols charts to assess gain and phase margins; SISO cuts are performed at the generalized control variables with the other loops remaining closed
- Bode diagrams of the closed loop responses from command variables to associated output to analyze steady-state accuracy, closed-loop bandwidth, high frequency phase behavior and transient response amplitude peaks

Some of the most important results of the linear assessment are that meeting the challenging time-constant requirements leads to significant control activity at low dynamic pressures associated with decreasing stability margins. This result backs the requirement to define the handling qualities as a function of the flight condition in contrast to requiring constant behavior over the whole flight envelope. The high responsiveness and agility that can easily be achieved at high dynamic pressures cannot be produced with the required stability reserves at low dynamic pressures. Extending the dynamics that is possible at low speeds over the whole envelope would unnecessarily limit the maneuverability of the aircraft far below its physical capabilities which are to be fully exploited for system specific maneuvers like low altitude flying. Another important result of the linear analysis is also the trade-off between pitch attitude dropback and bandwidth of the stick to flight-path angle transfer function.

The pilot in the loop simulations performed so far have successfully proven that the FCS design meets the specifications. Besides normal maneuvers, also formation flying and steep approaches have been performed.

The fast integrator philosophy has not produced any PIO tendencies so far, even during formation flying in the presence of turbulence. On the other hand, the fast integrators lead to a

quick and complete compensation of asymmetries, e.g. during simulated engine failures.

As far as pitch control is concerned, the presence of a head up display containing a flight-path marker leads to a pilot preference in high stick to flight-path angle response bandwidth in spite of significant associated attitude dropback. Thus the dropback reducing command shaping filter has been removed to account for this preference.

During rapid changes in thrust setting and the deployment of speedbrakes, the pitch control system slightly departs from the commanded flight-path angles indicating that the fast integrator might not be sufficient to attenuate the effect of those rapid control movements. This might indicate the requirement for additional feedforward compensations to eliminate the transient excursions, although they are small and become only apparent in clinical still air simulator conditions.

7 Conclusions and Perspectives

Although just intended for simulator use, significant efforts have been made to implement a realistic flight control system resembling the known or required characteristics of the configuration to be analyzed.

Much attention was drawn to a high level of automation as far as gain and coefficient design is concerned to account for the rapid changes in model data, fidelity as well as to the aim capability of rapidly analyzing the impact of changes in requirements.

So far, especially the pilot simulations have proven that the system is suitable for the tasks to be performed. The next interesting steps include analysis of specific maneuvers like low altitude flying and the role of envelope protections and limitations on performing such maneuvers. For example, one item will address the impact of pitch and bank angle limits during certain maneuvers. Furthermore, it is intended to add the simulation of an autothrust system as well as of basic autopilot modes.

8 References

[1] Brockhaus, R.: *Flugregelung*. Springer, Berlin, 1994.

[2] Heller, M.: *Untersuchung zur Steuerung und Robusten Regelung der Seitenbewegung von Hyperschall-Flugzeugen.* Herbert Utz Verlag, München, 1999.

[3] Faleiro, L.: *The Application of Eigenstructure Assignment to the Design of Flight Control Systems.* Doctoral Thesis, Loughborough University, 1998.

[4] Farineau, J.: *Lateral Electric Flight Control Laws of a Civil Aircraft Based upon Eigenstructure Assignment Technique*. Aerospatiale, Toulouse.

[5] Favre, C.: *Fly-by-wire for commercial:. The Airbus Experience.* International Journal of Control, 1994.

[6] Littleboy, D. M.: *Numerical Techniques for Eigenstructure Assignment by Output Feedback in Aircraft Applications.* University of Reading, Department of Mathematics, 1994.

[7] Satoh, A. and Sugimoto, K.: *Partial Eigenstructure Assignment Approach for Robust Flight Control.* Nara, Institute of Science and Technology. Journal of Guidance, Vol. 27, No. 1.

[8] Holzapfel F., da Costa O., Heller M. and Sachs G.: *Development of a Lateral-Directional Flight Control System for a New Transport Aircraft.* AIAA Guidance, Navigation, and Control Conference, Keystone, CO, August 2006.

[9] Holzapfel F., da Costa O., Heller M. and Sachs G.: *Development of a Longitudinal Control System for a New Transport Aircraft.* AIAA Guidance, Navigation, and Control Conference, Keystone, CO, August 2006.

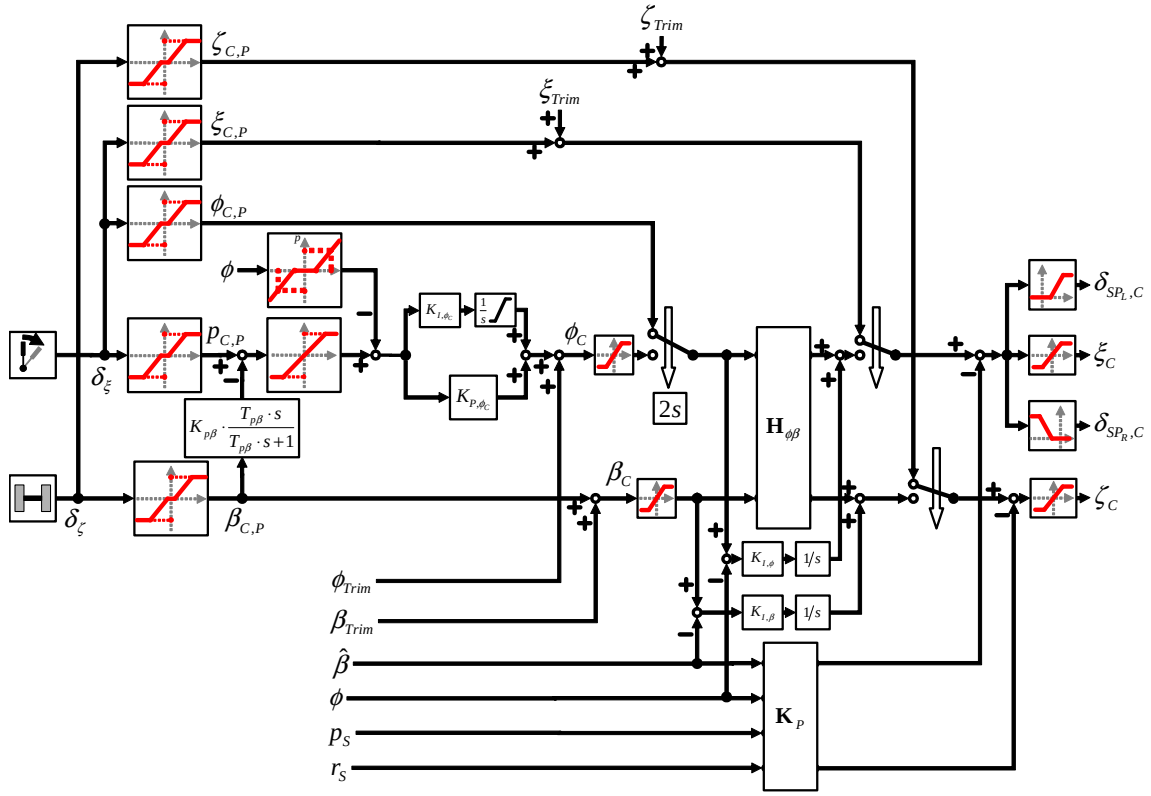

Fig.1 : Basic Layout of the Lateral-Directional Control System

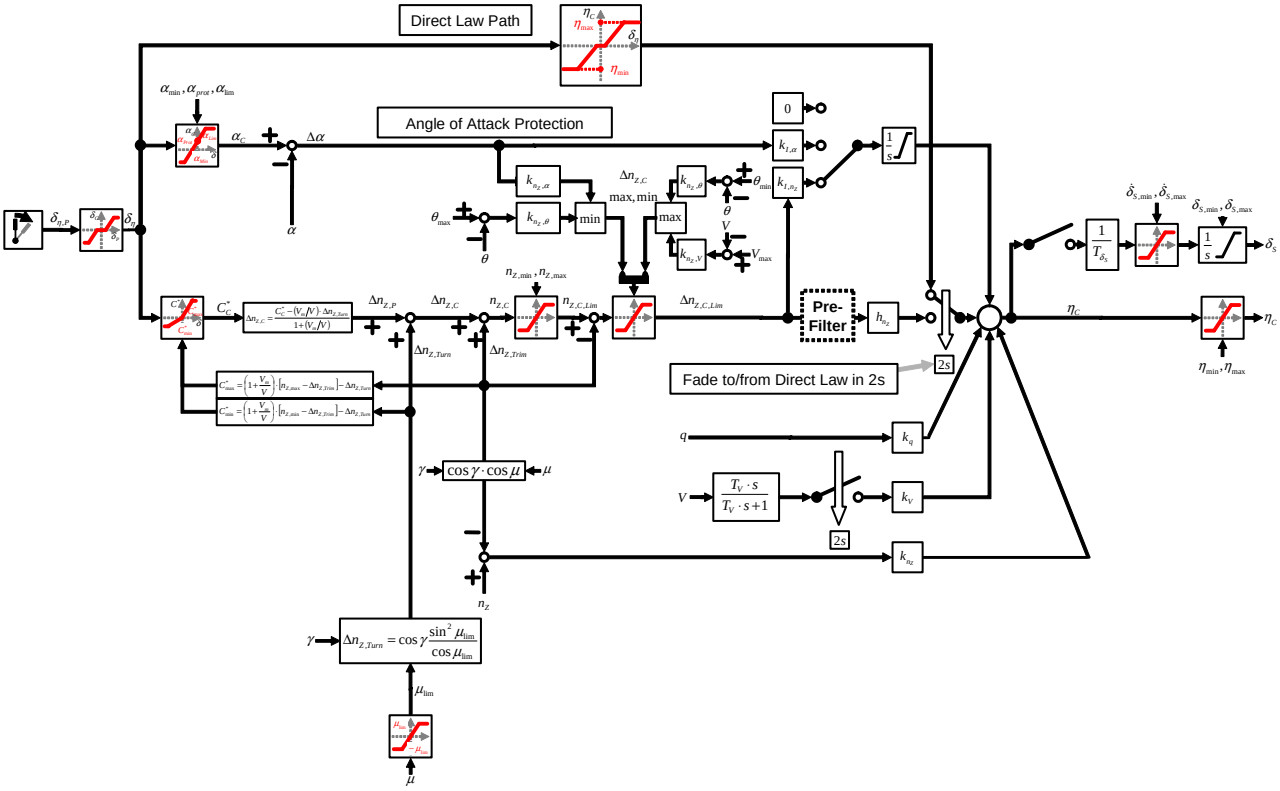

Fig.2 : Basic Layout of the Pitch Control System

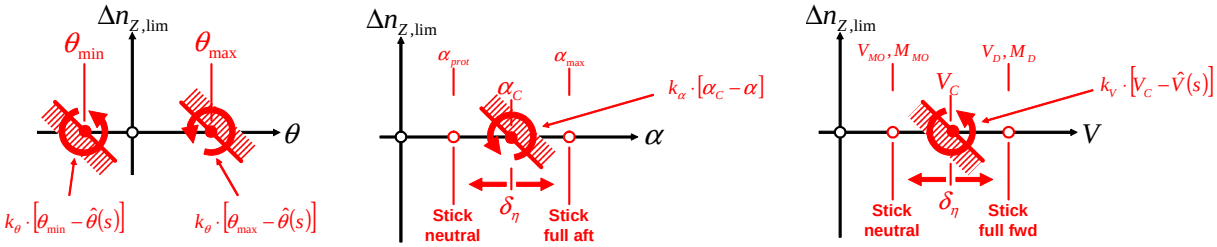

Fig.3 : Implementation of Limitations / Protections by Dynamic Command Limiting

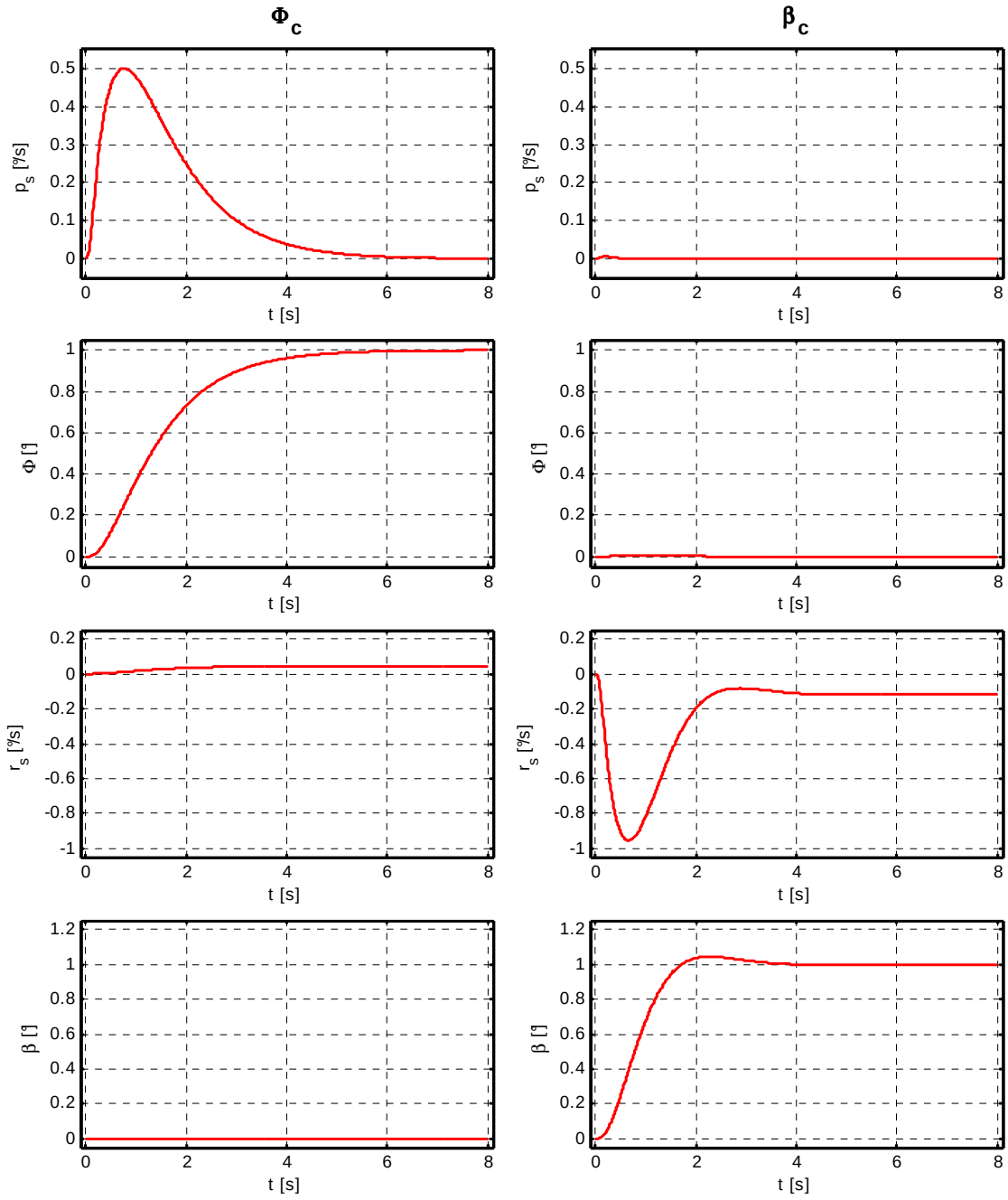

Fig.4 : Linear Step Response of Lateral Directional States